

1 **A family of transcription factors that limit lifespan:**

2 **ETS factors have conserved roles in longevity**

3

4 *Adam J. Dobson¹, Richard Boulton-McDonald¹, Lara Houchou¹, Ziyu Ren¹, Mimoza Hoti¹, Maria Rodriguez-*
5 *Lopez¹, Alexis Gkantiragas¹, Afroditi Gregoriou¹, Jürg Bähler¹, Marina Ezcurra², Nazif Alic^{1,3}*

6

7 1 – Institute of Healthy Ageing, Department of Genetics, Evolution and Environment, University College
8 London, Gower Street, London WC1E 6BT, UK.

9

10 2 – School of Biological and Chemical Sciences, Queen Mary University of London, London E1 4NS, UK.

11

12 3 – For correspondence: n.alic@ucl.ac.uk

13

ABSTRACT

14

15 Increasing average population age, and the accompanying burden of ill health, is one of the public health
16 crises of our time. Understanding the basic biology of the ageing process may help ameliorate the
17 pathologies that characterise old age. Ageing can be modulated, often through changes in gene expression
18 where regulation of transcription plays a pivotal role. Activities of Forkhead transcription factors (TFs) are
19 known to extend lifespan, but detailed knowledge of the broader transcriptional networks that promote
20 longevity is lacking. This study focuses on the E twenty-six (ETS) family of TFs. This family of TFs is large,
21 conserved across metazoa, and known to play roles in development and cancer, but the role of its
22 members in ageing has not been studied extensively. In *Drosophila*, an ETS transcriptional repressor, *Aop*,
23 and an ETS transcriptional activator, *Pnt*, are known to genetically interact with *Foxo* and activating *Aop* is
24 sufficient to extend lifespan. Here, it is shown that *Aop* and *Foxo* effect a related gene-expression
25 programme. Additionally, *Aop* can modulate *Foxo*'s transcriptional output to moderate or synergise with
26 *Foxo* activity depending on promoter context, both *in vitro* and *in vivo*. *In vivo* genome-wide mRNA
27 expression analysis in response to *Aop*, *Pnt* or *Foxo* indicated, and further experiments confirmed, that
28 combinatorial activities of the three TFs dictate metabolic status, and that direct reduction of *Pnt* activity is
29 sufficient to promote longevity. The role of ETS factors in longevity was not limited to *Pnt* and *Aop*.
30 Knockdown of *Ets21c* or *Eip74EF* in distinct cell types also extended lifespan, revealing that lifespan is
31 limited by transcription from the ETS binding site in multiple cellular contexts. Reducing the activity of the
32 *C. elegans* ETS TF *Lin-1* also extended lifespan, a finding that corroborates established evidence of roles
33 of this TF family in ageing. Altogether, these results reveal the ETS family of TFs as pervasive and
34 evolutionarily conserved brokers of longevity.

35

INTRODUCTION

36

37 Ageing is characterised by a steady systematic decline in biological function and increased
38 likelihood of disease. Understanding the basic biology of ageing therefore promises to help alleviate the
39 personal and societal burdens resulting from the increasing proportion of older people in our populations.
40 The pursuit of this goal has revealed that ageing is plastic, and healthy lifespan can be extended by
41 manipulating specific genes, including those encoding components of nutrient signalling pathways¹. Such
42 interventions often act through changes in gene expression, with transcriptional regulation playing a critical
43 role²⁻⁵. Sequence-specific transcription factors (TFs) are the primary coordinators of transcriptional
44 programmes⁶. Hence, understanding their function in adult animals will provide insight into how gene
45 expression can be altered to optimise physiology towards promoting lasting health into late life.

46 TFs can be classified into families based on their DNA-binding domains, reflecting common
47 evolutionary ancestry⁷. TFs of the forkhead family have been studied extensively in the context of ageing.
48 This large family of eukaryotic TFs can be further subdivided based on the sequence of their DNA-binding
49 domain (DBD), the forkhead box. Activation of Forkhead Box O (*Foxo*) orthologues in insects and
50 nematodes extends their lifespan, and alleles of *Foxo3* are associated with longevity in humans⁸⁻¹¹.
51 Furthermore, Foxos are required for the longevity achieved by the inhibition of the insulin/IGF signalling
52 (IIS) pathway in worms and flies^{12,13}. Foxos do not act in isolation, rather their outputs are tuned by the
53 activities of additional TFs. For example, the *C. elegans* Foxo, DAF-16, acts in concert with the heatshock
54 factor *HSF* and the GATA family TF *Elt-2* to regulate a pro-longevity transcriptional programme^{4,14}. Other
55 TFs are regulated by IIS in parallel to DAF-16, such as SKN-1, whose activity is sufficient to extend lifespan
56 independently of DAF-16¹⁵. The complex interactions observed between Foxos and these additional TFs
57 are best described as regulatory circuits which must be correctly coordinated to realise anti-ageing
58 transcriptional programmes.

59 The E twenty six (ETS) family of TFs, is conserved across animals, including 28 genes in
60 humans¹⁶⁻¹⁸. The shared, defining feature of ETS TFs is a core helix-turn-helix DBD, which binds DNA on
61 5'-GGA(A/T)-3' ETS-binding motifs (EBMs). These TFs are further classified into four subgroups based on
62 variation in peripheral amino acid residues, which confer binding specificity depending on nucleotide
63 variation flanking the core EBM. This binding specificity is thought to differentiate the transcriptional outputs
64 of distinct ETS TFs within the same cell¹⁹. In common with Foxos, ETS TFs generally function as

65 transcriptional activators, although a few have been shown to repress transcription^{20,21}. The *Drosophila*
66 *Aop* (a.k.a. *Yan*, the orthologue of human *Te1*) is an ETS TF that is thought to only act as a transcriptional
67 repressor.

68 The ETS family has been studied extensively in the context of cancer^{18,19}, but recent evidence
69 suggests a role in ageing. For example, AOP activation is associated with *Foxo*-mediated longevity in the
70 fruit fly, and AOP activation alone is sufficient to extend lifespan³. Additionally, in multiple organisms,
71 examination of the evolutionarily-conserved targets of Foxos has highlighted the conserved presence of
72 ETS-binding sites within regions bound by Foxo orthologues²², indicating that ETS factors may be
73 important participants in Foxo's longevity programme in a number of animals. Accordingly, in nematodes,
74 reducing the activity of *ets-4* extends lifespan, conditional on the presence of DAF-16²³. Clearly, wider
75 investigation of how ETS TFs determine lifespan is warranted.

76 This study set out to investigate transcriptional regulation by AOP. The study showed that *Aop* and
77 *Foxo* drive a common longevity transcriptional programme *in vivo* and interact to determine transcriptional
78 outcomes, both *in vitro* and *in vivo*. Additionally, *Aop* blocks transcriptional activation by *Pnt*, an ETS
79 transcriptional activator, and *in vivo* analysis of interactions between *Aop*, *Pnt* and *Foxo* indicated that the
80 key function of the common and coordinated transcriptional programme of *Foxo* and *Aop* for longevity is to
81 block the activity of *Pnt*. The transcriptomic analysis revealed, and further experiments confirmed, that
82 metabolism is modulated by the combined activity of the three TFs and that directly limiting *Pnt* activity was
83 sufficient to extend lifespan. These lifespan-regulatory effects were not confined to *Pnt* and *Aop*: limiting
84 the activities of further two ETS TFs in a range of tissues promoted longevity. The finding of a role in
85 ageing which is conserved in at least half of the ETS TFs in *Drosophila* suggests an evolutionarily ancient
86 origin. Consistent with this hypothesis, a previously unappreciated role in *C. elegans* longevity is shown for
87 the ETS TF *Lin-1*. Altogether these results reveal new functions of ETS TFs at the nexus of lifespan and
88 metabolism, opening up the investigation of these TF in adult physiology.

89

RESULTS

90

91 1) FOXO and AOP collaboratively establish a pro-longevity transcriptional programmes

92 *Aop* and its orthologue *Tel* are proposed to repress transcription by physical competition with
93 activators for binding sites^{20,24,25}, recruitment of additional repressive complexes^{21,25,26} and formation of
94 homo-oligomers to limit activator access to euchromatin²⁷⁻²⁹. Hence, to understand the role of *Aop* in
95 longevity, its interactions with relevant transcriptional activators need to be examined.

96 Foxo is one such transcriptional activator: both *Foxo* and *Aop* are required for longevity by IIS
97 inhibition, acting downstream of Pi3K-Akt or Ras-ERK pathways, respectively^{13,23}, where the shared
98 genomic locations bound by AOP and FOXO *in vivo* suggest that gene expression downstream of IIS is
99 coordinated by the orchestrated recruitment of FOXO and AOP to promoters. But what is the overall
100 relationship between the transcriptional programmes triggered by *Foxo* and *Aop*? The transcriptomic
101 response to induction of either *Foxo*, *Aop^{ACT}* (encoding a constitutively active form of AOP) or both, was
102 characterised in adult female fly guts and fat bodies (equivalent to mammalian liver and adipose), tissues
103 from which the two TFs extend lifespan³. The TF expression was under the control of the *S,106* driver,
104 induced by feeding the RU₄₈₆ inducer.

105 The transcriptional programmes triggered by *Foxo* or *Aop^{ACT}* were significantly correlated within the
106 set of 896 genes differentially regulated by either TF in the gut, or the equivalent 745 genes in the fat body
107 (Figure 1A-B; for details of differential expression analysis results see Supplementary Tables 1-8). Gene
108 Ontology (GO) enrichment analysis suggested that, in the gut, these shared targets were involved in
109 translation and energy metabolism (Supplementary Table 9), whilst the equivalent analysis in the fat body
110 suggested orchestration of genome regulation (Supplementary Table 10). Since the sets of differentially
111 expressed genes were largely tissue-specific (Supplementary Figure 1), this correlated response appeared
112 as a general feature of the *Foxo* and *Aop* regulons, independent of specific target promoters, in both the
113 gut and fat body. Hence, *Aop* and *Foxo* appear to act on lifespan through a shared transcriptional
114 programme.

115 FOXO and AOP exhibit extensive genomic co-localisation, with 60% of FOXO-bound loci also bound
116 by AOP in the adult female fly gut and fat body³. Does AOP directly modulate FOXO activity? To
117 investigate how AOP interacts with FOXO on a promoter to influence transcription, a series of
118 transcriptional reporters was constructed by combining the *Adh* basal promoter with FOXO-responsive

119 elements (FREs: AACAA), ETS-binding motifs (EBMs: GGAA) or both, and examined for their response to
120 FOXO and AOP^{ACT} in *Drosophila* S2 cells (Figure 1C). Neither FOXO nor AOP^{ACT} influenced reporter
121 expression in the absence of FREs, and FOXO alone was sufficient to activate transcription from the FREs,
122 confirming published observations^{24,30,31}. Combining the FREs and EBMs allowed AOP^{ACT} to attenuate the
123 activation by FOXO, revealing that AOP can moderate FOXO's activity when brought onto the same
124 promoter. By striking contrast, in the absence of EBMs, AOP^{ACT} synergised with FOXO to stimulate
125 induction from 20-fold by FOXO alone to 100-fold, indicating that AOP^{ACT} can accentuate FOXO's ability to
126 activate transcription. Since this synergy occurred in the absence of EBMs, this effect is most likely indirect.
127 Interestingly, this synergy may account in part for the strong similarity in AOP's and FOXO's transcriptional
128 programmes *in vivo*. Statistical modelling confirmed that the outcome of combining AOP and FOXO was
129 promoter-dependent (Supplementary Table 11). Hence, the presence or absence of EBMs determines
130 whether AOP functions to enhance or moderate FOXO activity on a promoter.

131 To examine if synergy and antagonism of *Foxo* by *Aop* can be observed on native promoters *in vivo*,
132 *Foxo* targets were tested for patterns of transcriptional alteration by co-induction of *Aop*^{ACT}, in the above-
133 described transcriptomic dataset. Overall, 55 were identified in the gut (Supplementary Table 12), and 179
134 in the fat body (Supplementary Table 13), whose modulation by *Foxo* was attenuated by *Aop*^{ACT} (Figure
135 1C). To determine the likely physiological outcomes of this inhibition of *Foxo* targets by *Aop*, GO
136 enrichment analysis was performed, revealing functions in lipid catabolism in the gut (Supplementary Table
137 14), and genome regulation in the fat body (Supplementary Table 15). No synergistic effects could be
138 detected in the fat body, but they could be discerned in the gut, where co-expressing both *Foxo* and *Aop*^{ACT}
139 led to differential expression of 1022 genes (Supplementary Table 16), which was not evident when either
140 TF was overexpressed alone (Figure 1E). GO enrichment analysis suggested that these synergistically-
141 regulated genes function in translation, proteolysis and mitochondrial regulation (Supplementary Table
142 17). Thus, transcript profiling confirmed that the two modes of AOP-FOXO interaction observed on
143 synthetic reporters can also occur *in vivo*. This simultaneous synergy and antagonism of AOP and FOXO
144 may explain why, while activation of each TF is sufficient to promote longevity, their co-activation does not
145 result in additive effect on lifespan³.

146

Figure 1

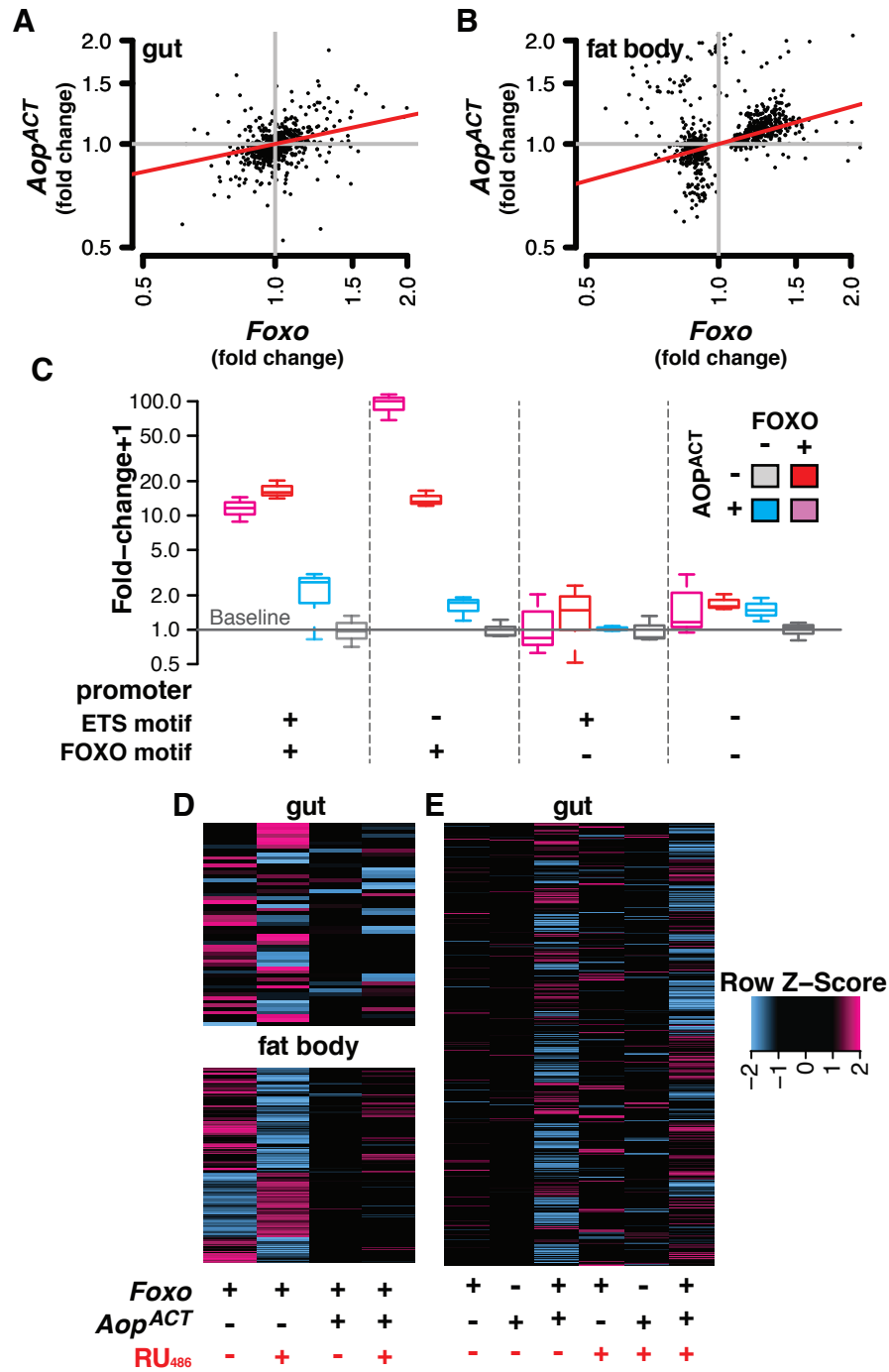


Figure 1. *Aop* recapitulates *Foxo*'s transcriptional output and modulates *Foxo* activity. Transcriptomic effects of *Aop*^{ACT} expression in **(A)** fly gut and **(B)** fat body correlate those of *Foxo* expression. RU₄₈₆-induced fold-changes in transcript abundance (relative to controls in the absence in RU₄₈₆) are shown, from the union of sets of genes differentially expressed in response to either or both TFs. Red lines show correlation coefficients (Kendall's Tau, $P \leq 2.2e-16$ for both tissues). **(C)** AOP^{ACT} both moderates and synergises transcriptional activation by FOXO on synthetic promoters containing combined ETS-binding motifs (EBMs) and FOXO-responsive elements (FREs), upstream of a basal *Adh-Firefly*^{luciferase} reporter. Activity is shown following normalisation to internal *Renilla*^{luciferase} controls, and calculation of fold-change over the median expression of each reporter in the absence of FOXO and AOP^{ACT}. See Supplementary Figure 2 for replicate experiment. *In vivo*, co-expressing *Aop*^{ACT} both **(D)** moderates the transcriptomic activity of *Foxo* in the fat body and gut, and **(E)** synergistically co-regulates transcription of distinct targets when co-expressed with *Foxo* in the gut. Values are shown as row-scaled Z values.

147 **2) *Pnt* modulates metabolism and limits lifespan**

148 Whilst interactions with FOXO likely account for some of the transcriptional outputs of AOP, 80% of
149 AOP-bound sites do not appear bound by FOXO *in vivo*³. Given the evidence that AOP alone is insufficient
150 to regulate transcription when brought onto a promoter (Figure 1C, and references^{20,23–29}, this observation
151 suggested that interactions with other TFs must account for the full breadth of AOP's physiological and
152 transcriptomic effects. One such TF is *Pnt*, whose activity is inhibited by *Aop* during fly development, which
153 is presumed to occur by competition for binding sites since the two recognise the same DNA sequence^{24,32–}
154 ³⁴. As previously reported^{24,35,36}, transcriptional induction by PNT^{P1} (a constitutively active isoform of *Pnt*;
155 references^{37–39}) was completely blocked by AOP^{ACT} (Figure 2A), suggesting that PNT inhibition may be a
156 key factor in *Aop*'s pro-longevity effect. To evaluate this possibility *in vivo*, the transcriptome-wide effects of
157 co-expressing *Aop*^{ACT}, *Pnt*^{P1} and *Foxo* in the gut and fat body were assessed. In the gut, 512 transcripts
158 appeared to be subject to the combinatorial, interactive effects of the three TFs, as were 622 in the fat body
159 (Supplementary Table 18-19, with genes regulated by over-expressing *Pnt*^{P1} alone in Supplementary Table
160 20-21). To reveal emergent transcriptional programmes in each tissue, principal component analysis (PCA)
161 was performed over the transcripts that were differentially regulated by the varying combinations of the
162 three TFs. Remarkably, the first principal component (PC) of differentially expressed genes in the gut
163 distinguished flies by published lifespan outcomes³ with short-lived flies expressing *Pnt*^{P1} alone or in
164 combination with *Foxo* at one end of the PC; long-lived flies expressing one or both *Foxo* and *Aop*^{ACT}
165 forming a distinct group at the other end of the PC; and *Aop*^{ACT} countering the effect of *Pnt*^{P1} to form an
166 intermediate group (Figure 2B). In the fat body, a similar grouping was apparent on the diagonal of PCs 1
167 and 2 (Figure 2C). To infer functional consequences of these distinct transcriptional programmes,
168 transcripts from the input set corresponding to the PCs were isolated and GO enrichment analysis
169 performed (Supplementary Tables 22-23; along with GO enrichment in full sets of differentially-expressed
170 genes: Supplementary Tables 24-25). This revealed a strong enrichment of genes with roles in energy
171 metabolism, whose expression was strongly correlated to the PCs (Supplementary Figure 3). Overall, a
172 combined view of the PCA and GO analysis predicted that: (1) the *Foxo-Aop-Pnt* circuit regulates
173 metabolism, and (2) inhibiting *Pnt*'s output promotes longevity.

174 To test the prediction that the *Foxo-Aop-Pnt* circuit regulates metabolism, the individual and
175 combined effects of the three TFs were tested on protein, TAG (triacylglyceride, the main energy store in
176 insects) and glucose. Feeding RU₄₈₆ to *S106* control flies did not affect TAG, protein or glucose content

177 (Supplementary Figure 4). Since body mass was subject to a complex interaction involving all three TFs
178 (Supplementary Figure 5, Supplementary Table 26), confounding per-fly quantification, protein, glucose
179 and TAG were normalised to body mass. Protein density was increased by *Foxo* overexpression, and this
180 effect was enhanced by *Pnt* co-expression (Supplementary Figure 6, Supplementary Table 27). *Foxo* and
181 *Aop^{ACT}* reduced TAG, but had no effect on glucose (Figure 2D). By contrast, flies over-expressing *Pnt^{P1}*
182 had moderately increased whole-body glucose, with no evidence of alterations to TAG in this experiment
183 (Figure 2D). Critically, the metabolic effects of each TF were highly dependent on the activities of the
184 others for both glucose and TAG levels, as well as overall body mass, which was confirmed with statistical
185 analyses (Supplementary Tables 26 and 28-29). Overall, metabolite profiling revealed a tripartite dialogue
186 between the three TFs, in which distinct combinations have unique outcomes on metabolism, hence
187 confirming the physiological prediction from the transcriptomic analysis.

188 Since *Pnt* appeared to dictate the transcriptional outcomes that predicted metabolic regulation by
189 the *Foxo-Aop-Pnt* circuit, the role of *Pnt* in responses to nutritional stress was further evaluated. TAG was
190 quantified after a week of *Pnt* over-expression, and then after a subsequent six days of starvation. *Pnt^{P1}*
191 over-expression increased the loss of TAG induced by starvation (Figure 2E), suggesting that PNT
192 activation predisposes flies to mobilise energy stores. This was associated with decreased resistance to
193 the starvation stress, with flies over-expressing *Pnt* dying 24% earlier on average (Figure 2F). The
194 observed ability of *Pnt* to promote catabolism of energy stores may be beneficial in the face of over-
195 nutrition, and relevant to the Western human epidemic of metabolic disease associated with energy-rich
196 diets. A *Drosophila* model of such energy-rich diets is increasing dietary sugar. Flies fed a 40% sugar diet
197 die substantially earlier than controls fed a 5% sugar diet, and accumulate TAG⁴⁰⁻⁴². However *Pnt^{P1}*
198 overexpression restored TAG levels in flies on a high-sugar diet to those observed on a low-sugar diet
199 (Figure 2G). Whilst there was no statistically significant interaction of sugar and *Pnt^{P1}* induction in a linear
200 model (Supplementary Table 31), the adipogenic effect of sugar was opposed by *Pnt*, such that TAG levels
201 on a high sugar-diet with RU₄₈₆ were equivalent to those on a low-sugar diet without RU₄₈₆ (t-test: t=0.01,
202 p=0.99). Moreover, *Pnt^{P1}* induction spared flies from the full extent of the early death induced by dietary
203 sugar, increasing median survival time by 26%, despite having no effect on the low-sugar diet (Figure 2H).
204 Note that in two of three experiments performed, and consistent with published data³, the induction of *Pnt^{P1}*
205 reduced the basal levels of TAG (Figure 2E and 2G). Altogether, these results suggest that complex

206 interactions in the *Foxo-Aop-Pnt* circuit determine homeostatic set-points for nutrient storage; and that *Pnt*
207 predisposes flies to leanness, which correlates survival of nutritional stress.

208 But what is the role of *Pnt* under healthy, nutritionally-optimal conditions? The attenuation of *Pnt*'s
209 transcriptomic effects by *Aop* indicated that limiting *Pnt* activity directly may be sufficient to extend lifespan.
210 To directly reduce *Pnt*, a validated⁴³ loss-of-function p-element insertion in *Pnt* (*Pnt*^{KG04968}, henceforth
211 *Pnt*^{KG}), was backcrossed into an outbred, wild-type background for ten generations. The mutation was
212 homozygous lethal. However, heterozygote females exhibited a 20% increase in median lifespan (Figure
213 2I). Similarly, inducing RNAi against *Pnt* from day three of adulthood in the gut and fat body also increased
214 lifespan (Figure 2J). The HMG-box repressor *capicua* (*cic*) represses expression of ETS factors including
215 *Pnt*⁴⁴ and, consistent with the effects of *pnt*^{RNAi}, overexpressing *cic*^{ΔC2} (a *cic* mutant lacking a known MAPK
216 phosphorylation site) in the gut and fat body also substantially extended lifespan (Figure 2K). This further
217 confirmed the functional predictions from the transcriptomic analysis and demonstrated that countering *Pnt*,
218 in the tissues in which *Foxo* and *Aop* over-expression is beneficial, is sufficient to extend lifespan.

219

220

Figure 2

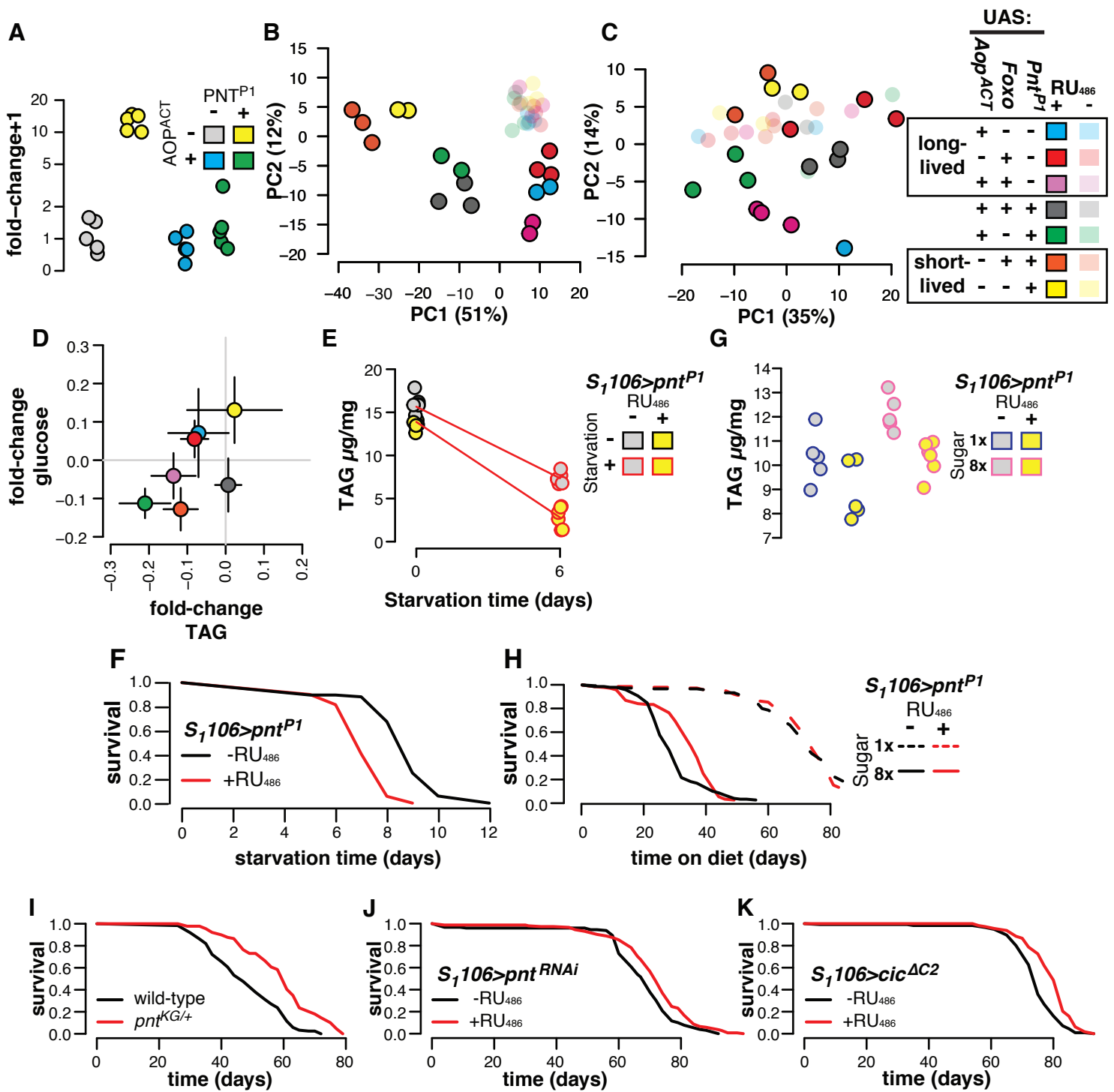


Figure 2. *Pnt* brokers transcriptomic, metabolic and longevity outcomes (A) AOP^{ACT} counteracts activation by PNT^{P1} of a synthetic promoter containing ETS-binding motifs, upstream of an *Adh-Fireflyluciferase* reporter. Activity is shown following normalisation to internal *TK-Renilla* *luciferase* controls, and calculation of fold-change over median expression in the absence of PNT^{P1} and AOP^{ACT}. Promoter activation was subject to a significant AOP^{ACT}:PNT^{P1} interaction (ANOVA $F_{1,16}=41.725$, $p=7.9e-6$) **(B-C)** Aggregate transcriptional effects of *Aop*^{ACT} counter those of *Pnt*^{P1} to establish transcriptional programs corresponding to lifespan. For gut and fat body, plots show coordinates of samples on the first two dimensions of principle components analysis, amongst transcripts which were differentially expressed according to combined TF co-expression (significant genotype:RU₄₈₆ interaction). Legend shows samples' groupings by previously-published lifespan outcomes resulting from TF induction in the gut and fat body or the gut alone (noting that lifespan effects of combined *Aop*^{ACT} and *Pnt*^{P1} expression are not known)³. **(D)** Metabolites are determined by a three-way interaction of *Pnt*, *Aop* and *Foxo*. Axes show glucose and TAG per unit body mass, expressed as fold-change (mean±SE) in the presence of RU₄₈₆, relative to the corresponding RU₄₈₆-negative genotype control. Both TAG and glucose were subject to statistically significant interactions of *Foxo***Aop*^{ACT}**Pnt*^{P1} induction (Supplementary Tables 20-21). **(E)** Over-expressing *Pnt*^{P1} in the gut and fat body accelerates loss of TAG under starvation stress. (ANOVA RU₄₈₆:starvation $F_{1,19}=7.03$, $p=0.02$. Full statistical analysis in Supplementary Table 30). **(F)** Over-expressing *Pnt*^{P1} in the gut and fat body reduces survival under starvation stress. The plot shows 71 deaths with RU₄₈₆, 68 deaths without, $p=1.3E-14$ (log-rank test). **(G)** Over-expressing *Pnt*^{P1} in the gut and fat body reduces accumulation of TAG on a high-sugar diet. *Pnt*^{P1} reduced TAG (ANOVA $F_{1,17}=14.4$, $p=1.4e-3$), sugar increased TAG ($F_{1,17}=15.25$, $p=1.1e-3$), with *Pnt*^{P1} appearing to counteract the effect of sugar (mean±SE: control 10.31±0.48, high sugar * RU₄₈₆ 10.30±0.29; t-test $t=0.009$, $p=0.99$, Full statistical analysis in Supplementary Table 31). **(H)** Over-expressing *Pnt*^{P1} in the gut and fat body enhances survival on a high-sugar diet. Plot shows 139 deaths and 3 censors on high sugar with RU₄₈₆ feeding (median=33.5 days), 146 deaths and 1 censor on high sugar without RU₄₈₆ feeding (median=26.5 days), 133 deaths and 17 censors on low sugar with RU₄₈₆ feeding (median=73 days), 122 deaths and 28 censors on low sugar without RU₄₈₆ feeding (median=71 days; Cox Proportional Hazards RU₄₈₆:diet $p=6e-3$; Full statistical analysis in Supplementary Table 32). **(I)** Heterozygous *Pnt* mutants are long-lived. Plot shows 122 wild-type deaths (median=45.5 days), 89 *pnt*^{KG/+} deaths (median=59.5 days), log-rank test $p=9.2e-11$. **(J)** Adult-onset *Pnt* inhibition in the gut and fat body is sufficient to extend lifespan. Plot shows 132 deaths and 19 censors without RU₄₈₆ feeding (median=68.5 days), 139 deaths and 16 censors with RU₄₈₆ feeding

(median=71 days), log-rank test $p=7.2e-4$. **(K)** Overexpression of *Cic*, a transcriptional repressor of *Pnt*, is sufficient to extend lifespan. Plot shows 113 deaths and 9 censors without RU₄₈₆ feeding (median=73.5 days), 113 deaths and 8 censors with RU₄₈₆ feeding (median=78.5 days), log-rank test $p=1.5e-7$.

221 **3) Modulating the activity of multiple ETS factors in multiple tissues and distinct species extends** 222 **lifespan**

223 Animal genomes encode multiple ETS factors. In *Drosophila* the ETS family comprises *Aop* and
224 *Pnt* along with six other ETS TFs (*Ets21c*, *Ets65A*, *Eip74EF*, *Ets96B*, *Ets97D*, *Ets98B*), each of which is
225 expressed with its own unique tissue-specific pattern (Supplementary Figure 7). The presumed common
226 ancestry of these TFs, along with their tissue-specific expression, suggests that they may regulate common
227 functions in distinct or partially-overlapping tissues, in which case roles in longevity may extend beyond
228 *Aop* and *Pnt*. *Cic*, whose overexpression extended lifespan (Figure 2K), represses both *Pnt* and *Ets21C*⁴⁴,
229 suggesting that *Ets21C* may also limit lifespan. Similar to *pnt^{RNAi}* and *cic^{ΔC2}*, inducing *Ets21C^{RNAi}* in the gut
230 and fat body with *S,106* extended lifespan (Figure 3A). Furthermore, both heterozygous and homozygous
231 mutants of *Ets21C* (bearing *Ets21C^{f03639}*, henceforth *Ets21C^F*, an intronic P-element insertion which was
232 backcrossed 10 times into wild-type flies) were also long-lived relative to controls (Figure 3B). Thus,
233 lifespan limitation is conserved between *Pnt* and *Ets21c*.

234 Are *Ets21c* and *Pnt* relevant to lifespan in the same tissues? To target a subset of the gut and fat
235 body cells marked by *S,106*, both TFs were knocked down specifically in enterocytes using the inducible,
236 enterocyte-specific driver *GS5966*. *Pnt* knockdown in enterocytes alone was still sufficient to extend
237 lifespan (Figure 3C). However, expressing *Ets21c^{RNAi}* with the same driver had no effect on longevity in
238 these cells (Figure 3D). This specificity appeared to reflect tissue-specific lifespan-limiting function of *Pnt*,
239 rather than differences in expression, since *Ets21c* is more highly expressed in these cells than *Pnt*⁴⁵,
240 therefore suggesting a level of tissue specificity in ETS TFs' effects on ageing. In this case, knocking down
241 diverse ETS factors in diverse tissues might be expected to extend lifespan.

242 *Pnt* is of known relevance to neurophysiology⁴⁶, especially in neurogenesis, and its continued
243 expression in adults⁵ suggests an ongoing physiologically-relevant role in neurons. However, expressing
244 *Pnt^{RNAi}* in neurons using the *Elav-GS* driver did not affect lifespan (Figure 3E). To explore if other ETS TFs
245 might be relevant to lifespan in neurons, *Eip74EF* was targeted by neuronal RNAi, because it is more
246 highly expressed in adult brain than in any other tissue (Supplementary Figure 7). We found that this
247 intervention also extended lifespan (Figure 3F). Hence, the *Drosophila* ETS family includes at least four
248 TFs with roles in ageing (*Aop*, *Pnt*, *Ets21C*, *Eip74EF*), and with distinct lifespan-limiting effects in specific
249 tissues.

250 The ETS TFs act downstream of receptor tyrosine kinase pathways^{13,44}. We also found some
251 evidence that different RTKs limit longevity in different cells: inducing the dominant-negative form of the
252 epidermal growth factor receptor (EGFR^{DN}) in enterocytes extended lifespan (Figure 3G), phenocopying
253 knockdown of *Pnt*, whereas the induction of the dominant-negative insulin receptor (InR^{DN}) did not (Figure
254 3H), whilst it is known to extend lifespan under control of other drivers¹⁰, and even though it is the more
255 highly expressed of the two RTKs in these cells⁴⁵. Hence, different ETS factors may limit lifespan
256 downstream of different RTK pathways.

257 Overall, we found evidence that the role in ageing is shared by multiple ETS factors in *Drosophila*.
258 ETS TFs are conserved throughout multicellular animals. The genome of the nematode *Caenorhabditis*
259 *elegans* encodes 11 in total. At least one of these, ETS-4, has been reported to limit lifespan in the worm
260 intestine²³. We found that the knockdown of one more, *Lin-1*, can also extend *C. elegans* lifespan (Figure
261 3I). Thus, multiple ETS factors limit lifespan across hundreds of millions of years of evolutionary
262 divergence, hinting at a general role for this family of TFs across animals.

Figure 3

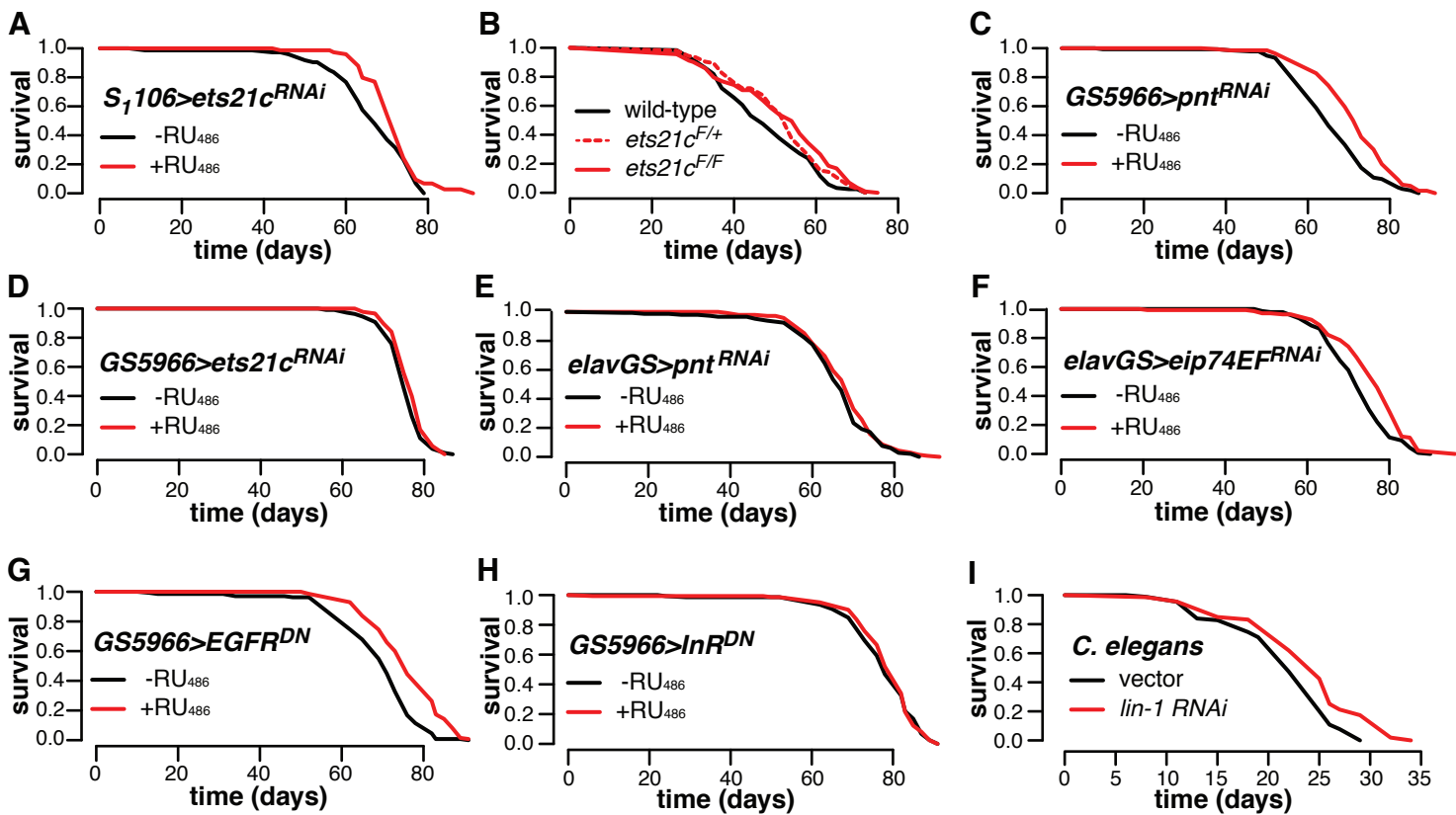


Figure 3. ETS transcription factors limit lifespan amongst diverse *Drosophila* tissues and across

species. (A) Knockdown of *Ets21c* by expressing *Ets21c^{RNAi}* in the gut and fat body extends lifespan. Plot shows 72 deaths and 1 censor without RU₄₈₆ feeding (median=65.5), 74 deaths and 1 censor with RU₄₈₆ feeding (median=71), $p=0.05$ (log-rank test). **(B)** Systematic *Ets21c* knockdown extends lifespan. Plot shows 122 wild-type deaths (median=45.5), 113 *Ets21c^{F/+}* deaths (median=52.5) and 104 *Ets21c^F/*Ets21c^F** deaths (median=52.5). Heterozygous $p=0.05$, homozygous $p=0.003$ (log-rank tests). Note that wild-type controls are also presented in Figure 2I. **(C)** Expressing *Pnt^{RNAi}* in enterocytes extends lifespan. Plot shows 121 deaths and 29 censors with RU₄₈₆ feeding (median=63.5), 127 deaths and 23 censors without RU₄₈₆ feeding (median=72), $p=7.33e-6$ (log-rank test). **(D)** Expressing *Ets21c^{RNAi}* in enterocytes does not affect lifespan. Plot shows 108 deaths and 12 censors without RU₄₈₆ feeding (median=73.5), 88 deaths and 17 censors with RU₄₈₆ feeding (median=76), $p=0.07$ (log-rank test). **(E)** Expressing *Pnt^{RNAi}* in neurons did not affect lifespan. Plot shows 140 deaths and 10 censors without RU₄₈₆ feeding (median=68.5), 146 deaths and 4 censors with RU₄₈₆ feeding (median=66), $p=0.27$ (log-rank test). **(F)** Expressing *Eip74E^{RNAi}* in neurons extends lifespan. Plot shows 140 deaths (and no censors) without RU₄₈₆ feeding (median=71), 134 deaths and 6 censors with RU₄₈₆ feeding (median=76), $p=6.73e-5$ (log-rank test). **(G)** Expressing a dominant-negative form of *EGFR* (*EGFR^{DN}*) in enterocytes extends lifespan. Plot shows 132 deaths and 16 censors without RU₄₈₆ feeding (median=70), 135 deaths and 15 censors with RU₄₈₆ feeding (median=74.5), $p=2.2e-9$ (log-rank test). **(H)** Expressing a dominant-negative form of *InR* (*EGFR^{DN}*) in enterocytes does not affect lifespan. Plot shows 127 deaths and 23 censors without RU₄₈₆ feeding (median=77), 134 deaths and 16 censors with RU₄₈₆ feeding (median=80), $p=0.66$ (log-rank test). **(I)** Knocking down *lin-1* in the nematode *C. elegans* extends lifespan. Plot shows 83 deaths and 6 censors with *lin-1^{RNAi}* feeding (median=25) and 100 deaths and 4 censors in vector-fed controls (median=22), $p=3.3e-2$.

263

DISCUSSION

264 Promoting lifespan by transcriptional control is an attractive prospect, because targeting one
265 specific protein can restructure global gene expression to reprogram physiology, orchestrating a cellular
266 recalibration that provides broad-scale benefits in ageing. This study suggests key roles for ETS TFs in
267 such optimisation. The results show dual roles for the ETS repressor *Aop* in longevity: balancing *Foxo*'s
268 outputs, whilst also opposing *Pnt*'s outputs. The outcome of this tripartite interaction is a program of
269 expression that corresponds to lifespan including genes with critical and conserved roles in central
270 metabolism. That directly reducing physiological *Pnt* is sufficient to extend lifespan suggests that
271 repressing transcription from the ETS site is the key longevity-promoting step in this circuit. Accordingly,
272 reducing transcription from the ETS site by targeting multiple TFs, in multiple *Drosophila* tissues, and in
273 multiple animal taxa, was sufficient to extend lifespan. Altogether, these results show that inhibiting lifespan
274 is a general feature of ETS transcriptional activators, and furthermore that this feature is conserved across
275 the ETS family.

276 The apparent lifespan-limiting role of ETS factors in adult animals is doubtlessly balanced by
277 selection for their important roles in development²⁴. There are at least two possible explanations for why
278 these TFs with detrimental long-term effects are active in adult tissues. ETS TF activity may simply run-on
279 from development, which may be neutral during the reproductive period (i.e. when exposed to selection)
280 but costly in the long term in aged animals. Additionally or alternatively, there may be context-dependent
281 benefits of activating transcription from the ETS site. This latter explanation is supported by two lines of
282 evidence: the enrichment of metabolic functions in the *Pnt* and *Aop* regulons suggests that metabolic
283 homeostasis is determined not by either TF alone, but by the balance of activation versus repression of
284 transcription from the ETS site, in which case benefits of *Pnt* activity would only be exposed in the face of
285 metabolic variation or stress. Fully consistent with the notion of context-dependent benefits of activating
286 transcription from the ETS site, the present data show that whilst *Pnt* is costly on a low-sugar diet, it can
287 improve survival on a high-sugar diet. The second line of evidence for context-dependent benefits of *Pnt* is
288 that, in mammals, different ETS TFs have distinct but partially-overlapping binding profiles^{16,19}, which may
289 indicate a shared set of core functions – perhaps in metabolism – which are important in response to
290 distinct signalling cues. In this case, the outcome of activating an ETS TF would depend on the fit between
291 promoter architecture and domains on the TF protein adjacent to the ETS domain. Indeed, the unexpected
292 recent finding that neuronal *Pnt* and *Aop* can have positively-correlated transcriptomic effects⁴⁷ is

293 consistent with highly context-dependent ETS TF function, likely subject to complex interactions of
294 euchromatin availability, a given TF's complement of protein domains, and the status of intracellular
295 signalling networks. This context-dependence makes it all the more remarkable that roles in lifespan
296 appear to be a conserved feature of the ETS TFs in diverse contexts.

297 Tissue environment appears to be a key contextual factor determining the effects of ETS TFs on
298 lifespan. This study shows that inhibiting distinct ETS TFs in multiple tissues is sufficient to extend lifespan.
299 Differences between tissues in chromatin architecture are likely to alter the capacity of a given ETS TF to
300 bind a given site. Indeed, whilst *Pnt* is of known neurophysiological importance, the lifespan extension
301 mediated by expressing RNAi against *Pnt* in the gut and fat body was not recapitulated by expressing the
302 same construct in neurons. By contrast, neuronal RNAi against *Eip74EF* was sufficient to extend lifespan,
303 and it has previously been implicated as a mediator of age-dependent functional decline⁴⁸. Similar tissue-
304 specific effects were evident in the matrix of *Pnt* and *Ets21c* knockdown in the gut and fat body versus the
305 gut alone. Furthermore, overexpression of dominant-negative receptor tyrosine kinases which are known to
306 act upstream of ETS TFs also had tissue-specific effects: over-expressing dominant-negative *EGFR^{DN}* in
307 enterocytes extended lifespan, whilst the equivalent expression of *InR^{DN}* did not, despite the status of both
308 receptors as activators of Ras/ERK signalling^{13,44}. This correspondence between the tissue-specific
309 outcomes of *Ets21c* and *InR* knockdown, and of *Pnt* and *EGFR* knockdown, suggests that lifespan-
310 promoting transcriptional programs may be inhibited by similar cellular signalling cascades across tissues,
311 such as *Pi3K-Akt* and *Ras-ERK*, but local regulation is coordinated by distinct receptors and TFs which
312 nevertheless ultimately converge on the ETS binding motif. It follows to ask whether inhibiting activation
313 from the ETS site in different tissues extends lifespan by alike cell-autonomous effects, or whether these
314 genetic lesions lead to cell-nonautonomous effects which are common across different tissues, giving an
315 organismal benefit that manifests in longevity. The relative importance in ageing of cell-autonomous versus
316 nonautonomous outputs of local transcriptional control remains to be established.

317 The structure of molecular networks and their integration amongst tissues underpins phenotype,
318 including into old age. This should be a key therapeutic consideration, as we attempt to bridge the gap
319 between genotype and specific age-related pathologies, such as dementia or cancer. Thus, unravelling the
320 basics of these networks is a critical step in identifying precise anti-ageing molecular targets¹. Perturbing
321 specific regulatory hubs can identify potential therapeutic targets, and identifying the least disruptive
322 perturbation of these networks, by targeting the “correct” effector, is a key goal in order to achieve desirable

323 outcomes without undesirable tradeoffs that may ensue from broader-scale perturbation. This targeting can
324 be at the level of specific proteins, specific cell types, specific points in the lifecourse, or a combination of
325 all three. The tissue-specific expression pattern of ETS TFs, and the apparent conservation of their roles in
326 longevity across distinct tissues, ETS family members and animal phyla, highlights them as important
327 regulators of tissue-specific programs, which may be beneficial in medically targeting both lifespan and
328 precise senescent pathologies.

329

MATERIALS & METHODS

330 *D. melanogaster* culture

331 All experiments were carried out in outbred, *Wolbachia*-free *Dahomey* flies, bearing the *w1118*
332 mutation and maintained at large population size since original domestication. All transgenes
333 (Supplementary Table 33) were backcrossed into this background at least 6 times prior to experimentation
334 and maintained without bottlenecking. Cultures were maintained on 10% yeast (MP Biomedicals, OH,
335 USA), 5% sucrose (Tate & Lyle, UK), 1.5% agar (Sigma-Aldrich, Dorset, UK), 3% nipagin (Chemlink
336 Specialities, Dorset, UK), and 3% propionic acid (Sigma-Aldrich, Dorset, UK), at a constant 25°C and 60%
337 humidity, on a 12:12 light cycle. Experimental flies were collected as embryos following 18h egg laying on
338 grape juice agar, cultured at standardised density until adulthood, and allowed to mate for 48h before
339 males were discarded and females assigned to experimental treatments at a density of 15 females/vial. To
340 induce transgene expression using the GeneSwitch system, the inducer RU₄₈₆ (Sigma M8046) was
341 dissolved in absolute ethanol and added to the base medium to a final concentration of 200 µM. Ethanol
342 was added as a vehicle control to RU-negative food. For lifespan experiments, flies were transferred to
343 fresh food and survival was scored thrice weekly. Feeding RU₄₈₆ to driver-only controls did not affect
344 lifespan (Supplementary Figure 8). For starvation stress experiments, flies were fed RU₄₈₆ or EtOH-
345 supplemented media for one week, before switching to 1% agarose with the equivalent addition of RU₄₈₆ or
346 EtOH, with death scored daily until the end. For sugar stress experiments, sugar content was increased to
347 40% w/v sucrose^{40–42}.

348

349 *C. elegans* culture

350 Worms were maintained by the protocol of Brenner⁴⁹, at 20°C on NGM plates seeded with
351 *Escherichia coli* OP50. For lifespan experiments, N2 (wildtype N2 male stock, N2 CGCM) were used at
352 20°C on NGM plates supplemented with 15µM FUDR to block progeny production. RNAi treatment was
353 started from egg. Animals that died from internal hatching were censored.

354

355 Molecular cloning

356 The *pGL3Basic-4xFRE-pADH-Luc* construct (called pGL4xFRE) described in reference³¹ was used
357 as template to generate PCR products containing 6xETS-4xFRE-pADH, 4xFRE-pADH, 6xETS-pADH- or

358 pADH (primers in Supplementary Table 34, ETS sequence as described by reference⁵⁰), flanked by *XhoI*
359 and *HindIII* sites, cloned into the corresponding sites in pGL3Basic and confirmed by sequencing.

360 *PntP1* was amplified from *UAS-PntP1* genomic DNA with Q5 High-Fidelity Polymerase (NEB
361 M0491S - primers in Supplementary Table 26) *Aop^{ACT}* was cloned from genomic DNA of *UAS-Aop^{ACT}* flies
362 as described in ³. *PntP1* and *Aop^{ACT}* sequences were then cloned into the *pENTR-D-TOPO* gateway vector
363 (Thermo 450218) before recombination into the *pAW* expression vector.

364

365 **S2 cell culture**

366 *Drosophila* S2 cells were cultured in Schneider's medium (Gibco/Thermo Scientific 21720024),
367 supplemented with 10% FBS (Gibco/Thermo Scientific A3160801) and Penicillin/Streptomycin (Thermo
368 15070063). Cells were split into fresh media 24h before transfection, then resuspended to a density of 10⁶
369 ml⁻¹ and transfected using Effectene reagent (Qiagen 301425) in 96-well plates, according to the
370 manufacturer's instructions. Reporters and TF expression plasmids were co-transfected with *pAFW-eGFP*
371 to visually confirm transfection, and *pRL-TK-Renilla^{luc}* as an internal control for normalisation of reporter-
372 produced Firefly luciferase. Reporter activity was measured 18h after transfection using Dual-Luciferase
373 reagents (Promega E1960). *pAHW-Foxo* and/or *pAW-Aop^{ACT}* were co-transfected with promoters bearing
374 combinations of FREs and EBMs. *pAW-Aop^{ACT}* and *pAW-PntP1* were co-transfected with a promoter
375 bearing EBMs.

376

377 **Transcriptomics**

378 Fly guts and fat bodies were dissected in ice-cold PBS and placed directly into ice-cold Trizol
379 (Ambion 15596026), from flies bearing combinations of *UAS-Foxo*, *UAS-Aop^{ACT}* and *UAS-PntP1* in an
380 *S1,06-GS* background, after six days adult feeding on RU₄₈₆. Three experimental replicates were sampled
381 for all conditions, each comprising a pool of twelve fat bodies or guts. RNA was extracted by Trizol-
382 chloroform extraction, quantified on a NanoDrop, and quality-assessed on an Agilent Bioanalyzer. Poly(A)
383 RNA was pulled down using NextFlex Poly(A) beads (PerkinElmer NOVA-512981). Samples with low
384 yields or low quality of RNA were excluded, leaving 2-3 replicate samples per experimental condition. RNA
385 fragments were given unique molecular identifiers and libraries were prepared for sequencing using
386 NextFlex qRNAseq v2 reagents (barcode sets C and D, PerkinElmer NOVA-5130-14 and NOVA-5130-15)

387 and 16 cycles of PCR. Individual and pooled library quality was assessed on an Agilent Bioanalyzer.
388 Sequencing was performed on an Illumina HiSeq 2500 instrument by the UCL Cancer Institute.

389

390 **Metabolic assays**

391 Metabolites were measured as per reference⁵¹ in whole adult flies after setting up the same fly
392 genotypes as for transcriptomics and an additional *S₁106/+* control, and following one week of RU₄₈₆
393 feeding. Flies were CO₂-anaesthetised, weighed on a microbalance, and immediately flash-frozen in liquid
394 N₂. To assay metabolites, flies were thawed on ice and homogenised by shaking with glass beads (Sigma
395 G8772) for 30s in a ribolyser at 6500 Hz in ice-cold TET buffer (10 mM Tris, 1 mM EDTA, 0.1% v/v Triton-X-
396 100). Aliquots of these homogenates were spun 1m at 4500g and 4°C to pellet debris, and re-frozen at -
397 80°C for protein quantification. Protein was assayed with the Bio-Rad Protein DC kit (Bio-Rad 5000112). A
398 second set of aliquots were heated to 72°C for 15m to neutralise enzymatic activity, before spinning and
399 freezing prior to triglyceride and carbohydrate assays. Triglyceride was measured by treating 10 µl sample
400 with 200 µl Glycerol Reagent (Sigma F6428) for 10m at 37°C and measuring absorbance at 540 nm, then
401 incubating with 50 µl Triglyceride Reagent (Sigma F2449) for 10m at 37°C and re-measuring absorbance at
402 540 nm, calculating glycerol content in each reading, then quantifying triglyceride content as the difference
403 between the first and second measurement. Glucose was measured on 5 µl homogenates with Infinity
404 reagent (Thermo TR15421) after 15m incubation at 37°C.

405

406 **Data analysis**

407 Sequence data were quality-checked by FastQC 0.11.3, duplicate reads were removed using Je
408 1.2, and reads were aligned to *D. melanogaster* genome 6.19 with HiSat2 2.1. Alignments were
409 enumerated with featureCounts 1.6. All downstream analyses were performed in R 3.3.1. The gut and fat
410 body were analysed in parallel. Transcripts with a mean <1 read count were excluded, leaving 11069 in the
411 fat body and 10366 in the gut (Supplementary Tables 35-36). Read counts are given in Supplementary
412 Tables 37-40. Differentially expressed (DE) genes were identified using DESeq2, at a false discovery rate
413 of 10%. Effects of RU₄₈₆ feeding were established in individual genotypes, and for specific analyses the
414 interactive effects of genotype and RU₄₈₆ were established. Sets of shared *Foxo* and *Aop^{ACT}* targets were
415 formed as the union of DE genes in *S106* flies over-expressing one or both transcription factors, following
416 RU₄₈₆ feeding. Epistatic interactions amongst TFs were identified by fitting models of the form

417
$$y^i \sim genotype + RU_{486} + block + genotype:RU_{486}$$

418 where *block* represented experimental replicate. The tripartite interaction of *Foxo*, *Aop^{ACT}* and *Pnt^{P1}* was
419 identified by applying the model to all genes across all experimental conditions, and isolating genes with a
420 significant *genotype:RU₄₈₆* term. Antagonism of *Foxo*'s outputs by *Aop^{ACT}* was identified by fitting the model
421 to samples of flies bearing either *UAS-Foxo* or both *UAS-Foxo* and *UAS-Aop^{ACT}*, on the subset of genes
422 which had already been identified as DE following *Foxo* over-expression. Synergistic effects of *Foxo* and
423 *Aop^{ACT}* were identified in the gut by fitting the model to all genes, from samples bearing either or both of the
424 *UAS-Foxo* and *UAS-Aop^{ACT}* transgenes. GO analysis was performed using the TopGO package, applying
425 Fisher's test with the *weight01* algorithm. Principal Components Analysis was performed on read counts of
426 these genes following a variance-stabilizing transformation. To characterise gene-expression correlates of
427 principal components, loadings onto principal components were extracted using the *dimdesc* function from
428 the *FactoMineR* library, and GO analysis performed as previously. Transcripts of genes annotated with
429 enriched GO terms were then plotted per term by centering variance-stabilised reads to a mean of zero and
430 plotting against PC values per sample. Heatmaps were plotted using the *heatmap.2* function from the
431 *gplots* library, ordering rows by hierarchical clustering by Ward's method on Euclidian distance, and scaling
432 to row.

433 Fly lifespan data were analysed using log-rank tests in Microsoft Excel. Worm lifespan data were
434 analysed by log-rank tests in JMP. Luciferase reporter data were normalised by taking the ratio of firefly
435 luciferase to renilla luciferase signal and, for each promoter, calculating fold-change for each sample
436 relative to the median activity of the promoter in the absence of FOXO and AOP^{ACT}. To assess the
437 interaction of FOXO and AOP with promoters' complements of TF-binding motifs, these normalised data
438 were analysed by fitting a linear model of the form

439
$$y \sim FRE * EBM * FOXO * AOP^{ACT}$$

440 in which *y* was the \log_N of fold-change+1, FRE and EBM represented the TF-binding complement, and
441 FOXO and AOP^{ACT} represented co-transfection with *pAHW-Foxo* or *pAW-Aop^{ACT}*. The interactive effect of
442 PNT^{P1} and AOP^{ACT} were assessed by fitting a linear model of the form

443
$$y \sim PNT^{P1} * AOP^{ACT}$$

444 The interactive effect of TFs on metabolites and body mass were analysed by normalising
445 metabolite density to fly mass, and then calculating fold-change for each experimental genotype in the

446 presence of RU_{486} relative to the mean in the absence of RU_{486} . These fold-change data per metabolite
447 were analysed by linear models of the form

448
$$y \sim Foxo * Pnt^{P1} * Aop^{ACT}$$

449 where each predictor encoded a binary term for the presence/absence of the TF. The effect of Pnt^{P1}
450 overexpression on TAG and lifespan responses to nutrient stress (starvation or high-sugar diet) were
451 analysed by a model of the form

452
$$y \sim RU_{486} * diet$$

453 where y represented TAG normalised to unit weight in a linear model, or survival in a Cox Proportional
454 Hazards model (survival library).

455

456

457

ACKNOWLEDGMENTS

458 We thank Danny Filer, Rita Ibrahim, Kami Shalfrooshan, Jeremie Subrini and Caesar Chi for technical
459 assistance; Oscar Puig, Rachel Hunt, Joeseeph Bateman, Cathy Slack and Ekin Bolukbasi for sharing
460 plasmids and cells; Bruce Edgar for sharing flies; Steve Parratt for analytical advice; and Jennifer Lohr for
461 conducting pilot experiments in *C. elegans*. This work was funded by BBSRC grant BB/M029093/1 and
462 Royal Society grant RG140694 to NA.

463

464

SUPPLEMENTARY FIGURE LEGENDS

465

466 **Figure S1.** Euler plot showing overlap between the unions of *Foxo* and *Aop*'s regulons in the gut and fat
467 body.

468 **Figure S2.** Replicate experiment of results shown in Fig 3c. Results were qualitatively consistent in each of
469 the two replicates: AOP^{ACT} both moderates and synergises with transcriptional activation by FOXO on
470 synthetic promoters containing combined ETS-binding motifs (EBMs) and FOXO-responsive elements
471 (FREs), upstream of a basal *Adh-Firefly^{luciferase}* reporter. Activity is shown following normalisation to internal
472 *Renilla^{luciferase}* controls, and calculation of fold-change over the median expression of each reporter in the
473 absence of FOXO and AOP^{ACT}. Statistical analysis in Supplementary Table 11.

474 **Figure S3.** Expression of transcripts subject to the 3-way *Foxo-Aop-Pnt* interaction, and annotated with
475 significantly enriched GO terms (the five categories with lowest enrichment p-values), plotted over the first
476 principal component of the expression matrix for each tissue (correlated to lifespan). Expression values
477 were derived by applying *DESeq2*'s variance-stabilising transformation to read counts, taking medians per
478 transcript, and mean-sweeping values. Principal component values are shown in Figure 2B-C.

479 **Figure S4.** Activating *Gal4* in the fat body and gut by feeding the inducer RU₄₈₆ to *S₁106/+* control flies
480 does not affect whole-body levels of TAG (t-test $t=-0.61$, $df=11.54$, $p=0.56$) or glucose (t-test $t=1.27$,
481 $df=13.98$, $p=0.22$). Data were collected in the same experiment as shown in Figure 2D.

482 **Figure S5.** Effects of *Foxo-Aop-Pnt* interactions on body mass per fly. X-axis labels indicate the
483 combination of overexpression constructs (e.g. "foxo,aop,pnt" denotes presence of *UAS-Foxo*, *UAS-Aop^{ACT}*
484 and *UAS-Pnt^{P1}*), with *S₁106* present in all cases. "+" indicates *S₁106*-only controls. Accompanying
485 statistical analysis is presented in Supplementary Table 26.

486 **Figure S6.** Effects of *Foxo-Aop-Pnt* interactions on protein content per unit fly weight. X-axis labels indicate
487 the combination of overexpression constructs (e.g. "foxo,aop,pnt" denotes presence of *UAS-Foxo*, *UAS-*
488 *Aop^{ACT}* and *UAS-Pnt^{P1}*), with *S₁106* present in all cases. "+" indicates *S₁106*-only controls. Accompanying
489 statistical analysis is presented in Supplementary Table 27.

490 **Figure S7.** Tissue-specific expression of ETS TFs. A variance-stabilising transformation was applied to
491 read counts (from⁵, from the same population of flies, on the same media) and medians were calculated.
492 Data were column-scaled so that the figure shows each TFs relative expression across tissues, and
493 hierarchically clustered using Ward's method on Euclidian distance.

494 **Figure S8.** Activating *Gal4* in the fat body by feeding the inducer RU₄₈₆ to *S₁106/+* control flies, or in
495 enterocytes in *GS5966/+* control flies, does not affect lifespan. *GS5966/+*: plot shows 125 deaths and 4
496 censors (median=71) without RU₄₈₆ feeding, 128 deaths and 6 censors with RU₄₈₆ feeding (median=73.5),
497 $p=0.08$ (log-rank test). *S₁106/+*: plot shows 123 deaths and 3 censors without RU₄₈₆ feeding
498 (median=73.5), 128 deaths and 6 censors with RU₄₈₆ feeding (median=73.5).

BIBLIOGRAPHY

- 499
500
- 501 1. Kenyon, C. J. The genetics of ageing. *Nature* **464**, 504–512 (2010).
- 502
- 503 2. Murphy, C. T. *et al.* Genes that act downstream of DAF-16 to influence the lifespan of
504 *Caenorhabditis elegans*. *Nature* **424**, 277–284 (2003).
- 505
- 506 3. Alic, N. *et al.* Interplay of dFOXO and Two ETS-Family Transcription Factors Determines
507 Lifespan in *Drosophila melanogaster*. *PLoS Genetics* **10**, (2014).
- 508
- 509 4. Hsu, A., Murphy, C. & Kenyon, C. Regulation of aging and age-related disease by DAF-16 and
510 heat-shock factor. *Science* **300**, 1142–1145 (2003).
- 511
- 512 5. Dobson, A. J. *et al.* Tissue-specific transcriptome profiling of *Drosophila* reveals roles for GATA
513 transcription factors in longevity by dietary restriction. *Npj Aging Mech Dis* **4**, 5 (2018).
- 514
- 515 6. Lambert, S., Jolma, A., Campitelli, L., Das, P. & Cell, Y.-Y. The human transcription factors.
516 *Cell* **172**, 650–665 (2018).
- 517
- 518 7. Pabo, C. O. & Sauer, R. T. Transcription Factors: Structural Families and Principles of DNA
519 Recognition. *Annual Review of Biochemistry* **61**, 1053–1095 (1992).
- 520
- 521 8. Morris, B. J., Willcox, D., Donlon, T. A. & Willcox, B. J. FOXO3: a major gene for human
522 longevity-a mini-review. *Gerontology* **61**, 515–525 (2015).
- 523
- 524 9. Flachsbar, F. *et al.* Association of FOXO3A variation with human longevity confirmed in
525 German centenarians. *Proc National Acad Sci* **106**, 2700–2705 (2009).
- 526

- 527 10. Bolukbasi, E. *et al.* Intestinal Fork Head Regulates Nutrient Absorption and Promotes
528 Longevity. *Cell Reports* **21**, 641–653 (2017).
529
- 530 11. Willcox, B. J. *et al.* FOXO3A genotype is strongly associated with human longevity. *Proc*
531 *National Acad Sci* **105**, 13987–13992 (2008).
532
- 533 12. Gems, D. *et al.* Two pleiotropic classes of daf-2 mutation affect larval arrest, adult behavior,
534 reproduction and longevity in *Caenorhabditis elegans*. ... **150**, 129–155 (1998).
535
- 536 13. Slack, C. *et al.* The Ras-Erk-ETS-Signaling Pathway Is a Drug Target for Longevity. *Cell* **162**,
537 72–83 (2015).
538
- 539 14. Zhang, P., Judy, M., Lee, S.-J. & Kenyon, C. Direct and Indirect Gene Regulation by a Life-
540 Extending FOXO Protein in *C. elegans*: Roles for GATA Factors and Lipid Gene Regulators. *Cell*
541 *Metab.* **17**, 85–100 (2013).
542
- 543 15. Tullet, J. *et al.* Direct Inhibition of the Longevity-Promoting Factor SKN-1 by Insulin-like
544 Signaling in *C. elegans*. *Cell* **132**, 1025–1038 (2008).
545
- 546 16. Hollenhorst, P. C., McIntosh, L. P. & Graves, B. J. Genomic and Biochemical Insights into the
547 Specificity of ETS Transcription Factors. *Annu Rev Biochem* **80**, 437–471 (2011).
548
- 549 17. Sharrocks, A. The ETS-domain transcription factor family. *Nature Reviews Molecular Cell*
550 *Biology* **2**, 827–837 (2001).
551
- 552 18. Sharrocks, A. D., Brown, A. L., Ling, Y. & Yates, P. R. The ETS-domain transcription factor
553 family. *International Journal of Biochemistry and Cell Biology* **29**, 1371–1387 (1997).

554

555 19. Wei, G.-H. H. *et al.* Genome-wide analysis of ETS-family DNA-binding in vitro and in vivo.

556 *The EMBO journal* **29**, 2147–60 (2010).

557

558 20. Mavrothalassitis, G. & Ghysdael, J. Proteins of the ETS family with transcriptional repressor

559 activity. *Oncogene* **19**, 6524–6532 (2000).

560

561 21. Wang, L. & Hiebert, S. TEL contacts multiple co-repressors and specifically associates with

562 histone deacetylase-3. *Oncogene* **20**, 3716–25 (2001).

563

564 22. Webb, A. E., Kundaje, A. & Brunet, A. Characterization of the direct targets of FOXO

565 transcription factors throughout evolution. *Aging Cell* **15**, 673–685 (2016).

566

567 23. Thyagarajan, B. *et al.* ETS-4 Is a Transcriptional Regulator of Life Span in *Caenorhabditis*

568 *elegans*. *PLoS Genetics* **6**, e1001125 (2010).

569

570 24. O'Neill, E. M., Rebay, I., Tjian, R. & Rubin, G. M. The activities of two Ets-related transcription

571 factors required for *Drosophila* eye development are modulated by the Ras/MAPK pathway. *Cell*

572 **78**, 137–147 (1994).

573

574 25. Chakrabarti, S. R. & Nucifora, G. The Leukemia-Associated Gene TEL Encodes a

575 Transcription Repressor Which Associates with SMRT and mSin3A. *Biochemical and Biophysical*

576 *Research Communications* **264**, 871–877 (1999).

577

578 26. Guidez, F. *et al.* Recruitment of the nuclear receptor corepressor N-CoR by the TEL moiety of

579 the childhood leukemia-associated TEL-AML1 oncoprotein. *Blood* **96**, 2557–61 (2000).

580

- 581 27. Lopez, R. *et al.* TEL is a sequence-specific transcriptional repressor. *The Journal of biological*
582 *chemistry* **274**, 30132–8 (1999).
- 583
- 584 28. Qiao, F. *et al.* Derepression by depolymerization; structural insights into the regulation of Yan
585 by Mae. *Cell* **118**, 163–73 (2004).
- 586
- 587 29. Webber, J. L. *et al.* The relationship between long-range chromatin occupancy and
588 polymerization of the Drosophila ETS family transcriptional repressor Yan. *Genetics* **193**, 633–49
589 (2012).
- 590
- 591 30. Baker, D. A., Mille-Baker, B., Wainwright, M. S., Ish-Horowicz, D. & Dibb, N. J. Mae mediates
592 MAP kinase phosphorylation of Ets transcription factors in Drosophila. *Nature* **411**, 330–334
593 (2001).
- 594
- 595 31. Puig, O., Marr, M. T., Ruhf, L. M. & Tjian, R. Control of cell number by Drosophila FOXO:
596 downstream and feedback regulation of the insulin receptor pathway. *Genes & Development* **17**,
597 2006–2020 (2003).
- 598
- 599 32. Rebay, I. & Rubin, G. Yan functions as a general inhibitor of differentiation and is negatively
600 regulated by activation of the Ras1/MAPK pathway. *Cell* **81**, 857–66 (1995).
- 601
- 602 33. Lai, Z. & Rubin, G. Negative control of photoreceptor development in Drosophila by the
603 product of the yan gene, an ETS domain protein. (1992).
- 604
- 605 34. Lachance, J.-F. *et al.* A comparative study of Pointed and Yan expression reveals new
606 complexity to the transcriptional networks downstream of receptor tyrosine kinase signaling.
607 *Developmental biology* **385**, 263–278 (2013).

608

609 35. Vivekanand, P., Tootle, T. L. & Rebay, I. MAE, a dual regulator of the EGFR signaling
610 pathway, is a target of the Ets transcription factors PNT and YAN. *Mechanisms of development*
611 **121**, 1469–79 (2004).

612

613 36. Tootle, T. L., Lee, P. S. & Rebay, I. CRM1-mediated nuclear export and regulated activity of
614 the Receptor Tyrosine Kinase antagonist YAN require specific interactions with MAE.
615 *Development* **130**, 845–857 (2003).

616

617 37. Klaes, A., Menne, T., Stollewerk, A., Scholz, H. & Klämbt, C. The Ets transcription factors
618 encoded by the *Drosophila* gene pointed direct glial cell differentiation in the embryonic CNS. *Cell*
619 **78**, 149–160 (1994).

620

621 38. Klämbt, C. The *Drosophila* gene pointed encodes two ETS-like proteins which are involved in
622 the development of the midline glial cells. *Development (Cambridge, England)* **117**, 163–76
623 (1993).

624

625 39. Scholz, H., Deatrick, J., Klaes, A. & Genetics, K. C. Genetic dissection of pointed, a
626 *Drosophila* gene encoding two ETS-related proteins. (1993).

627

628 40. Dobson, A. J. *et al.* Nutritional Programming of Lifespan by FOXO Inhibition on Sugar-Rich
629 Diets. *Cell reports* **18**, 299–306 (2017).

630

631 41. Saud, S., Summerfield, A. C. & Alic, N. Ablation of insulin-producing cells prevents obesity
632 but not premature mortality caused by a high-sugar diet in *Drosophila*. *Proceedings of the Royal*
633 *Society of London B: Biological Sciences* **282**, 20141720 (2015).

634

- 635 42. Mair, W., Goymer, P., Pletcher, S. D. & Partridge, L. Demography of dietary restriction and
636 death in *Drosophila*. *Science* **301**, 1731–1733 (2003).
- 637
- 638 43. Maixner, A., Hecker, T. P., Phan, Q. N. & Wassarman, D. A. A screen for mutations that
639 prevent lethality caused by expression of activated sevenless and ras1 in the *Drosophila* embryo.
640 *Dev Genet* **23**, 347–361 (1998).
- 641
- 642 44. Jin, Y. *et al.* EGFR/Ras Signaling Controls *Drosophila* Intestinal Stem Cell Proliferation via
643 Capicua-Regulated Genes. *PLoS genetics* **11**, e1005634 (2015).
- 644
- 645 45. Dutta, D. *et al.* Regional Cell-Specific Transcriptome Mapping Reveals Regulatory Complexity
646 in the Adult *Drosophila* Midgut. *Cell Reports* **12**, 346–358 (2015).
- 647
- 648 46. Zhu, S., Barshow, S., Wildonger, J., Jan, L. & Jan, Y.-N. Ets transcription factor Pointed
649 promotes the generation of intermediate neural progenitors in *Drosophila* larval brains.
650 *Proceedings of the National Academy of Sciences* **108**, 20615–20620 (2011).
- 651
- 652 47. Duncan, O. F. *et al.* Ras-ERK-ETS inhibition alleviates neuronal mitochondrial dysfunction by
653 reprogramming mitochondrial retrograde signaling. *PLoS genetics* **14**, e1007567 (2018).
- 654
- 655 48. Liu, N. *et al.* The microRNA miR-34 modulates ageing and neurodegeneration in *Drosophila*.
656 *Nature* **482**, 519–525 (2012).
- 657
- 658 49. Brenner, S. The genetics of *Caenorhabditis elegans*. *Genetics* (1974).
- 659
- 660 50. Rogers, E. M. *et al.* Pointed regulates an eye-specific transcriptional enhancer in the
661 *Drosophila* hedgehog gene, which is required for the movement of the morphogenetic furrow.

662 *Development* **132**, 4833–4843 (2005).

663

664 51. Dobson, A. J. *et al.* Host genetic determinants of microbiota-dependent nutrition revealed by

665 genome-wide analysis of *Drosophila melanogaster*. *Nature Communications* **6**, 6312 (2015).

666